American Journal of Modern Energy
2015; 1(2): 44-51
Published online July 1, 2015 (http://www.sciencepublishinggroup.com/j/ajme)
doi: 10.11648/j.ajme.20150102.13

Numerical Study of Combined Natural Convection and Radiation in Three Dimensional Solar Thermal Collector: Focus on the Inclination Effect on Heat Transfer

Kaouther Ghachem[1], Mohamed Bechir Ben Hamida[2, 3], Chamseddine Maatki[1], Lioua Kolsi[1, 4], Mohamed Naceur Borjini[1], Habib Ben Aissia[1]

[1]Research Unit of Metrology and Energy Systems, National Engineering School, Energy Engineering Department, University of Monastir, Monastir city, Tunisia
[2]High School of Sciences and Technology of Hammam Sousse (ESSTHS), Department of Physics, University of Sousse, Sousse, Tunisia
[3]Research Unit of Ionized Backgrounds and Reagents Studies (UEMIR), Preparatory Institute for Engineering Studies of Monastir (IPEIM), University of Monastir, Monastir city, Tunisia
[4]College of Engineering Mechanical Engineering Department, Haïl University, Saudi Arabia

Email address:

kaouther_ghachem@yahoo.fr (K. Ghachem), benhamida_mbechir@yahoo.fr (M. B. B. Hamida), maatkichems@yahoo.fr (C. Maatki), lioua_enim@yahoo.fr (L. Kolsi), borjinimn@yahoo.com (M. N. Borjini), habib_enim@hotmail.fr (H. B. Aissia)

To cite this article:

Kaouther Ghachem, Mohamed Bechir Ben Hamida, Chamseddine Maatki, Lioua Kolsi, Mohamed Naceur Borjini, Habib Ben Aissia. Numerical Study of Combined Natural Convection and Radiation in Three Dimensional Solar Thermal Collector: Focus on the Inclination Effect on Heat Transfer. *American Journal of Modern Energy*. Vol. 1, No. 2, 2015, pp. 44-51. doi: 10.11648/j.ajme.20150102.13

Abstract: This paper studies the effect of the combined natural convection and radiation on the heat transfer and this, in an inclined solar thermal collector. A 3D numerical code is developed to solve respectively the convection equations according to the vorticity-vector potential formulation and the radiation equation. The discretize schema is the control volume method for the convection and the FTnFVM for the radiative equation. Numerical solutions are obtained for Pr=0.71, Ra=10^5, and the radiation-conduction parameter (rc) ranging from 0 to ∞. The medium is considered as gray. Indeed, it emits and absorbs heat.

Keywords: Natural Convection, Radiation, Inclinaned Cavity, Solar Collector

1. Introduction

Coupling of natural convection and radiation is prevalent in many industrial applications and natural phenomena. We quote for example: solar collectors, fire research, and building construction and insulation systems.

Many researchers have had a great interest to study pure natural convection in an inclined cavity. Mention may be made of the work of Ozoe, Sayama and Churchill [11] from one side and Ozoe, Yamamoto and Churchill [12] from the other side who reported that if the cavity is seriously inclined (ϕ between 80° and 90°), complex flow pattern with 3D multiple roll-cells would appear in the cavity. Wang Q.W, Wang, G., Zeng and Ozoe [14] studied the natural convection in 2D cavity with an inclined angle varying between 0° and 80°.

Recently, Henderson, Junaidi, Muneer, Grassie and Currie [8] conducted a review paper about the works in pure natural convection and pure radiation for inclined cavity.

It is worth noting that the first numerical study in literature about the coupled heat transfer problem involving both convection and radiation in a rectangular cavity seems to be that of Larson and Viskanta [9]. They found that radiation heats up the cavity surface and the gas body very quickly and thus considerably modifies the flow pattern and the corresponding convection process. Several two-dimensional studies are found for the problem of combined radiation and natural convection in rectangular participating medium (Chang, Yang and Lloyd [5]; Yang [16], Yucel, Acharya and Williams [1]) but many works take only into account the effects of surface-to-surface radiation in order to reduce computational effort (Balaji and Venkateshan [4] and Velusamy, Sundararajan, Seetharamu [13]), Chang , Yang and Lloyd [5] investigated combined radiation and natural convection in two-dimensional enclosures with partitions. Desreyaud and Lauriat [7] computed natural convection and radiation in rectangular enclosures using a one-dimensional P-1 radiation analysis. Webb and Viskanta [15] measured the natural convection induced by irradiation and compared experimental results with

the results of an analysis based on a spectral one-dimensional radiation model. A review paper on this subject was given by Yang [16]. A 3D numerical simulation of radiation and convection in a differentially heated cubic cavity using the discrete ordinates method is effectuated by Colomer, Costa, Cònsul and Oliva [6]. The authors detail the effect of the Planck number and the optical thickness on heat transfer and effectuate a comparison between dimensional results obtained from a two-dimensional model and those obtained in the mid-plane of a long rectangular enclosure. Later, Borjini, Mbow and Daguenet [2] studied numerically the effect of the radiative heat transfer on the three-dimensional convection in a cubic differentially heated cavity for different optical parameters of the medium, Pr = 13.6 and Ra=105. Their results show that the structure of the main flow is considerably altered by of the conduction–radiation parameter. Indeed, they found that the inner spiraling flows were very sensible in location and direction to the radiative heat transfer. However, the peripheral spiralling motion was qualitatively insensitive to these parameters. It is also found that radiation favorites the merging of the vortices near the front and back walls. Recently, Kolsi, Abidi, Maatki, Borjini, and Ben Aissia [10] studied the effect of radiative transfer and the aspect ratio on the 3D natural convection. Prandtl and Rayleigh numbers are respectively fixed at 13.6 and 105. They found that the principal flow structure is considerably modified when the radiation-conduction parameter was varied. However, the peripheral spiraling motion is qualitatively insensitive to these parameters. In all these works, radiation is found to play an important and sometimes major role in heat transfer and fluid flow processes.

In the present paper, we further study the combined radiation and natural convection in an inclined 3D cavity filled with emitting, absorbing, and isotropically scattering fluid. The work will be divided into two main parts, namely: effect of Rayleigh number on heat transfer and cavity inclination effect on the flow and heat transfer.

2. Mathematic Formulation

Figure1, presents the considered physical system which is composed of a square basic parallelepipedic enclosure, with aspect ratio F=H/W equal to 2. The two vertical walls are kept respectively at constant cold temperature and hot temperature. All the other walls are kept adiabatic. In the present study, the cavity is inclined around with an angle γ. All these surfaces are gray and diffuse. Even more, the cavity is filled with a gray, emitting–absorbing and isotropically scattering fluid. The flow is supposed to be laminar and the Boussinesq approximation is used. The dimension equations describing the combined radiation and natural convection are respectively:

Continuity:

$$\nabla.\vec{V}' = 0 \tag{1}$$

Momentum:

$$\frac{\partial \vec{V}'}{\partial t'} + (\vec{V}'.\vec{\nabla})\vec{V}' = -\frac{1}{\rho}\vec{\nabla}P' + \nu\Delta\vec{V}' + \beta_t(T' - T_0)\vec{g} \tag{2}$$

Energy:

$$\frac{\partial T'}{\partial t'} + \vec{V}'.\nabla T' = \alpha\nabla^2 T' - \frac{1}{\rho c_p}\vec{\nabla}q' \tag{3}$$

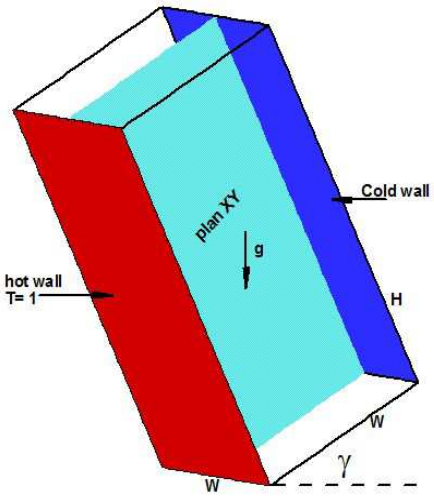

Fig. 1. *Physical models for: vertical cavity γ=0° (left) and inclined cavity 0°<γ<90° (right).*

As numerical method we had used the vorticity-vector potential formalism $(\vec{\psi} - \vec{\omega})$. This allows, in a 3D configuration, the elimination of the pressure, which is a delicate term to treat. For this, one applies the rotational to the equation of momentum (Eq.2). The vector potential and the vorticity are, respectively, defined by the two following relations:

$$\vec{\omega}' = \vec{\nabla}\times\vec{V}' \text{ and } \vec{V}' = \vec{\nabla}\bar{\times}\vec{\Psi}' \tag{4}$$

The foregoing dimensionless parameters are given as follow: time t' , velocity $\vec{V}'$, the vector potential $\vec{\psi}'$, the vorticity $\vec{\omega}'$, are put respectively in their dimensionless forms by W^2/α , α/W , α and W^2/α . The adimensional temperature is defined by: $T = (T' - T_c')/(\overline{T_h}' - T_c')$. Whereas $\overline{T_h}'$ is the mean temperature of the hot wall.

The system of equations controlling the phenomenon becomes:

$$-\vec{\omega} = \nabla^2\vec{\psi} \tag{5}$$

$$\frac{\partial\vec{\omega}}{\partial t} + (\vec{V}.\nabla)\vec{\omega} - (\vec{\omega}.\nabla)\vec{V} = \Delta\vec{\omega} + Ra.\Pr.\left[-g.\cos\gamma\frac{\partial T}{\partial z}; -g.\sin\gamma\frac{\partial T}{\partial z}; -(g\cos\gamma\frac{\partial T}{\partial x} + g\sin\gamma\frac{\partial T}{\partial y})\right] \tag{6}$$

$$\frac{\partial T}{\partial t}+\vec{V}.\nabla T=\nabla^2 T+\frac{Rc.\tau}{\Phi_t.\pi}(1-\omega_0).\left[\int_{4\pi} I.d\Omega-4.\pi.(1+\Phi_t T)^4\right] \quad (7)$$

Pr	is the Prandtl number	$Pr=\nu/\alpha$
Ra	is the Rayleigh number	$Ra=\frac{g\beta_t.W^3.(T_h-T_c)}{\alpha.\nu}$
Rc	is the radiation conduction parameter	$Rc=i^2.W.T_c'^3.\sigma/\lambda$
τ	is the optical width	$\tau=\kappa.W$
ϕt	is the temperature ratio	$\Phi_t=\overline{T_h}'/\overline{T_c}'-1$

The initial and boundary conditions are as follows:
Temperature

At x=0, T=1 and at x=1, T=0. On the other walls, $\frac{\partial T}{\partial n}=0$

Velocity: $V_x=V_y=V_z=0$ on all walls

Vorticity

$\omega_x=0 \quad \omega_y=-\frac{\partial V_z}{\partial x} \quad \omega_z=\frac{\partial V_y}{\partial x}$ at x=0 and 1

$\omega_x=\frac{\partial V_z}{\partial y} \quad \omega_y=0 \quad \omega_z=-\frac{\partial V_x}{\partial y}$ at $y=0$ and 1

$\omega_x=-\frac{\partial V_y}{\partial z} \quad \omega_y=\frac{\partial V_x}{\partial z} \quad \omega_z=0$ at z=0 and 1

Vector potential

$\frac{\partial \psi_x}{\partial x}=\psi_y=\psi_z=0$ at $x=0$ and 1

$\psi_x=\frac{\partial w_y}{\partial y}=\psi_z=0$ at $y=0$ and 1

$\psi_x=\psi_y=\frac{\partial \psi_z}{\partial z}=0$ at $z=0$ and 1

Radiative flux

$-\frac{\partial T}{\partial y}+q_r Rc/\Phi=0$ at y=0 and y=1

$-\frac{\partial T}{\partial z}+q_r Rc/\Phi=0$ at z=0 and z=1

The radiative transfer equation, for a gray semi-transparent medium which absorbs, emits and isotropically diffuses the radiation, can be viewed in the manuscript of Borjini, Mbow and Daguenet [2] et Kolsi, Abidi, Maatki, Borjini, and Ben Aissia [10].

3. Validation Test

The comparison of radiative and conductive fluxes on the heated wall, with the results of Colomer, Costa, Cònsul and Oliva [6] is presented, for several optical thicknesses, in Table 1. A remarkable difference is observed between the two results. This is a consequence that Colomer, Costa, Cònsul and Oliva [6] used the discrete ordinates method with suitable directions and for the classical 3D furnace case they compared their results only with the approximation P3 of the spherical harmonics.

Comparison of thermal transfer on the hot face between our results and those of the literature for Pr=0.71, Rc=1/(0.016×17) et Φt=1/17.

Table 1. *Comparison of thermal transfer on the hot face between our results and those of the literature for Pr=0.71, Rc=1/(0.016×17) et Φt=1/17.*

		τ = 0		**τ = 1**		**τ =10**	
		$\overline{q}_c$	$\overline{q}_r$ **rc/Φt**	$\overline{q}_c$	$\overline{q}_r$ **rc/Φt**	$\overline{q}_c$	$\overline{q}_r$ **rc/Φt**
Ra = 10^3	Our results	1.06	6.49	1.70	4.61	1.65	1.25
	Colomer et al.	1.76	6.20	1.76	4.64	1.54	1.16
Ra = 10^4	Our results	2.04	6.89	2.45	5.12	2.23	1.65
	Colomer et al.	2.26	6.28	2.25	4.69	2.11	1.54
Ra = 10^5	Our results	4.13	7.23	4.04	5.88	4.46	2.99
	Colomer et al.	4.37	6.52	3.92	5.44	4.21	2.8

4. Results and Discussion

To extract simulations for the present study, the parameters of simulations are respectively: a times step equal to10^{-4}, a space grid of 41x81x41 for F=2 and an angular grid FT6FVM.The Rayleigh number is fixed at 10^5 and the Prandtl number at 0.71. The optical with τ is equal to 1, Φt=0.1 and albedo equal to 1. The effects of the conduction-radiation parameter, the inclination angle of cavity and the oscillatory excitation on the principal flow and the heat transfer are discussed.

A. Effect of the variation of the Ra number on heat transfer

This section is reserved to show the influence of the Ra number on the heat transfer. Figure 2 shows that the increase of the Ra number and consequently the effect of natural convection, do not alter the average radiative flux. For the rest of the results the Ra number is fixed at 10^5.

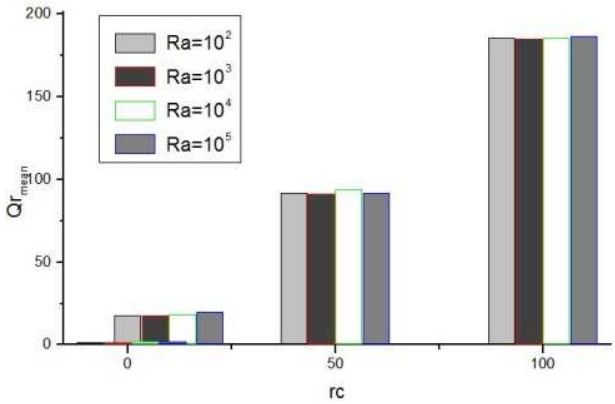

Fig. 2. *Effect of the Ra number on the mean radiative flux.*

B. Cavity Inclination effect on the flow and heat transfer

As shown in Figure 1, the cavity is gradually inclined with a step equal to 30°around z-axis. Four angles presented here are respectively: γ=0°, γ=30°, γ=60° and γ=90°. In these cases, the effect of γ is carefully investigated with the variation of the conduction-radiation parameter rc which evolved from 0 to infinite.

Figure 3 represents the projection of flow lines in the main plan XY for γ=0°. When rc=0 (Figure 3(a)), the flow is characterized by one thermal vortex slightly titled towards the cold wall and turns counter the clockwise. The streamlines are not closed and they form a spiral. When rc=10 (Figure 3(b)), the vortex moves toward the hot wall and stabilizes in the center of the cavity. For rc->∞ (Figure 3 (c)), one center vortex is shown and streamlines are closed.

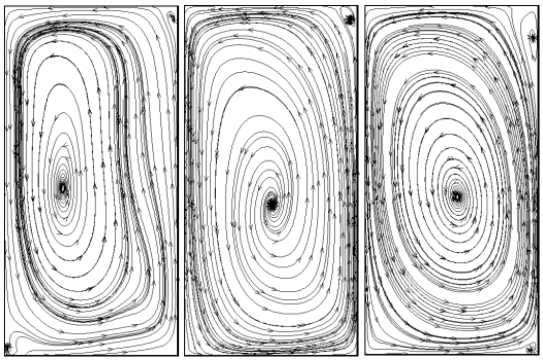

(a) (b) (c)

Fig. 3. *Projection of flow lines on the mid XY plan for γ=0° and rc respectively equal to 0 (a), 10 (b) and ∞ (c).*

Figure 4 represents the projection of flow lines in the main plan XY for γ=30°. For rc= 0 (Figure 4(a)), one vortex situated in the center of the cavity turns counter the clockwise. When rc= 10 (Figure 4(b)), one notes the apparition of one cell structure with three inner vortexes. The two vortexes situated in the top and in the bottom of the cavity turn counter the clockwise however the third one, situated in the center, turns in the clockwise. When rc->∞ (Figure 4(c)), these vortex disappear and one center vortex takes place. In this case, one notes the apparition of one small vortex in the top corner near the hot wall of the cavity turning in the clockwise.

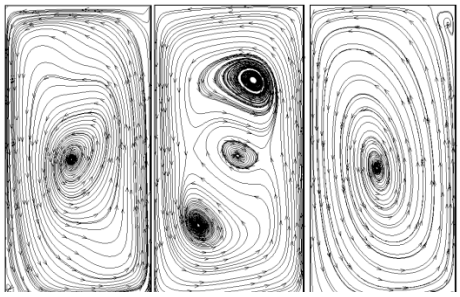

(a) (b) (c)

Fig. 4. *Projection of flow lines on the mid XY plan for γ=30° and rc respectively equal to 0 (a), 10 (b) and ∞ (c).*

Figure 5 represents the projection of flow lines in the main plan XY for γ=60°. In absence of radiation (Figure 5 (a)), one notes the apparition of one cell with three inner vortexes. The top and the bottom vortex are slightly titled to the cold wall and turn counter clockwise. The central vortex turns in the clockwise. For rc=10 (Figure 5(b)) one notices the coalescence of the three vortex and one vortex, slightly titled to the hot wall, takes place and turns counter the clockwise. By the increasing of rc which tends to infinite (Figure 5(c)), one center vortex appears and turns in the clockwise. For γ=90° (Figure 6) the problem of Rayleig-Benard convection is retrieved. Figure 6 shows the projection of the flow lines on the mid XY plane for rc=1, rc=10 and rc->∞. When rc=1 (Figure 6(a)) and rc= 10 (Figure 6(b)), two contra-rotative cells take place and when rc->∞ the flow presents height roll-cells. This result is earlier demonstrated by Ozoe et al. [11].

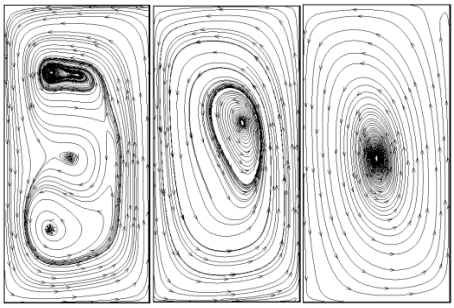

(a) (b) (c)

Fig. 5. *Projection of flow lines on the mid XY plan for γ=60° and rc respectively equal to 0 (a), 10 (b) and ∞ (c).*

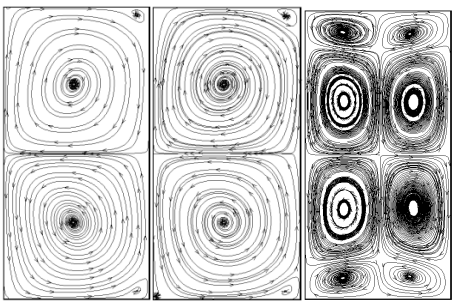

(a) (b) (c)

Fig. 6. *Projection of flow lines on the mid XY plan for γ=90° and rc respectively equal to 0 (a), 10 (b) and ∞ (c).*

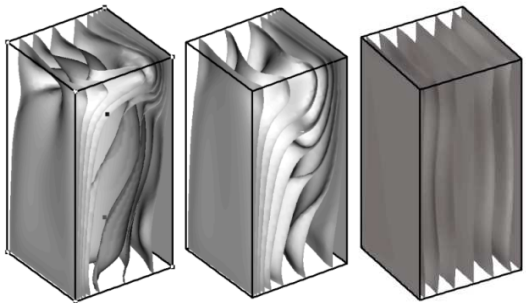

(a) (b) (c)

Fig. 7. *isothermal surfaces for γ=0° and rc respectively equal to 0 (a), 10 (b) and ∞ (c).*

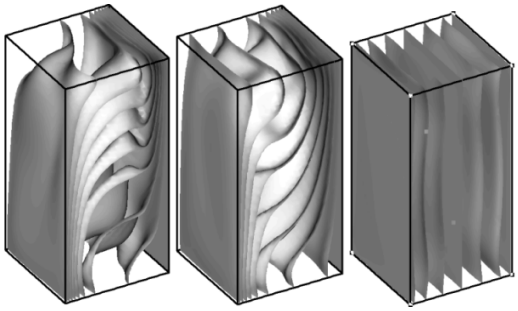

(a) (b) (c)

Fig. 8. *isothermal surfaces for γ= 30° and rc respectively equal to 0 (a), 10 (b) and ∞ (c).*

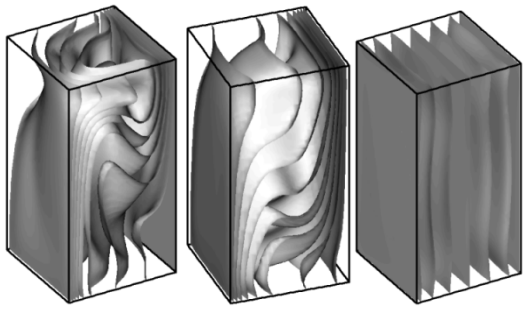

(a) (b) (c)

Fig. 9. *isothermal surfaces for γ=60° and rc respectively equal to 0 (a), 10 (b) and ∞ (c).*

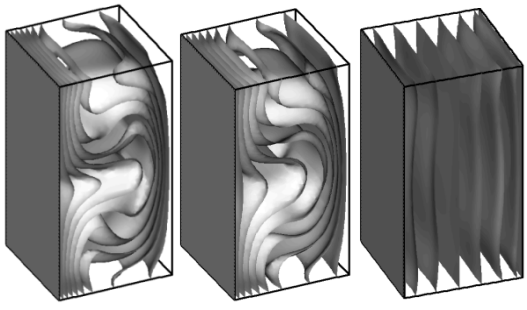

(a) (b) (c)

Fig. 10. *isothermal surfaces for γ=90° and rc respectively equal to 0 (a), 10 (b) and ∞ (c).*

The (Figure 7, Figure 8, Figure 9 and Figure 10) present the isothermal surfaces respectively for γ=0°, γ =30°, γ =60° and γ= 90°. In absence of radiative transfer (rc=0), and by increasing the inclination angle, one notes that the distribution of the isothermal surfaces is largely modified. In fact, isothermal surfaces are distorted and a 3D aspect appears in the core of the cavity. When the effect of the radiation increases rc=10, a vertical stratification appears in the core of the cavity and the thermal gradient decreases in the bottom near the hot wall and in the top near the cold wall. When rc goes to infinity the radiative heat transfer prevails and the isotherms are parallel to isothermal walls. Furthermore, one notes the 3D distribution of the temperature for low rc number. However for higher value of rc, the temperature field becomes independent of the flow and pure radiative transfer takes place. It should be noted that the inclination of the cavity has no effect on the temperature distribution when the conductive radiative parameter goes to infinity. In fact, the isothermal surfaces shown earlier in (Fig. (8(c), 9(c) and 10(c))), are identical and equidistant expected near active sides and they are symmetrical about the middle plane.

Figure 11 shows the evolution of mean radiative flux as a function of the angle of tilt for rc=10 and Ra $=10^5$. The inclination of the cavity minimizes the average value of the radiative flux which knows its minimum value to an angle close to 60 °. An inclination greater than 80° increases the average radiant flux which reaches its highest values.

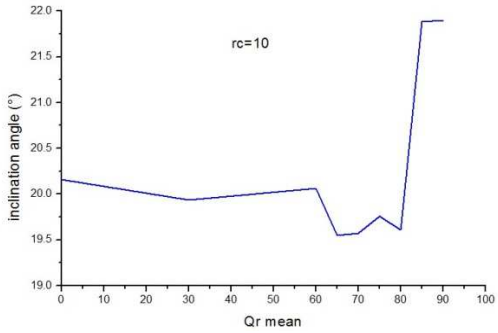

Fig. 11*. effect of inclination on radiative transfer (Qr mean) for rc=10.*

The distribution of the mean radiative flux along the Y direction shows an almost identical look for an inclination angle of the cavity, below 80°. When the configuration becomes similar to the Rayleigh-Benard case, the distribution of mean radiative flux is characterized by two extrema (Figure 12).

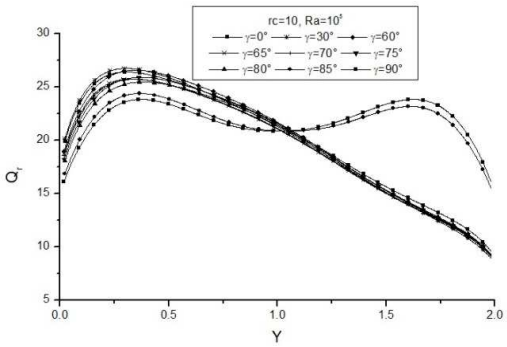

Fig. 12. *profile of Qr in Y direction for different inclination angle (rc=10 and Ra=10^5).*

The distributions of conductive and radiative heat fluxes on the hot wall are represented (Figure 13 and Figure 14) for the different inclinations angles and for rc=10. It is remarkable that for γ=0°, radiation increases conductive heat transfer at the top of the hot wall and decreases it at the bottom. Due to the temperature levels, the radiative flux is higher on the hot wall while the conductive flux is more important on the cold wall. These characteristics are qualitatively similar to those obtained in 3D by Colomer et al. [6] and 2D Tan and Howell, (1991) computations.

By increasing the inclination angle of the cavity, it is remarkable that the maximum values of the conductive heat transfer decrease (Figure 13) and those of the radiative heat transfer increases (Figure 14).

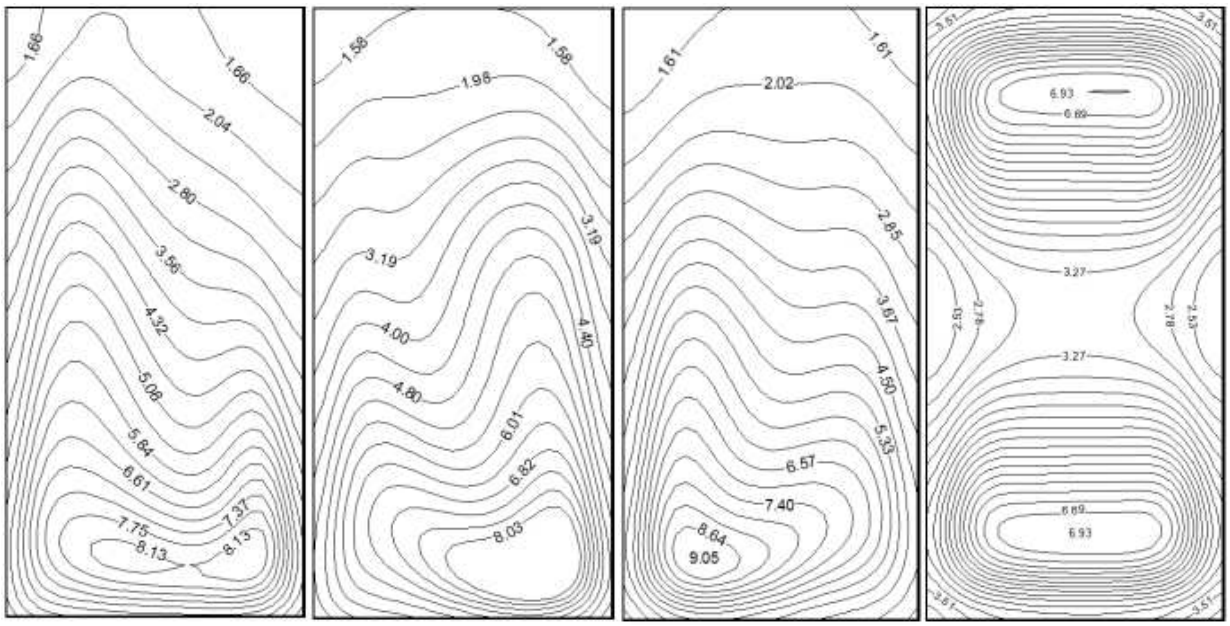

(a) (b) (c) (d)

Fig. 13. *Conductive fluxes distribution on the hot wall for rc=10 and γ=0° (a), 30° (b), 60°(c) and 90°(d).*

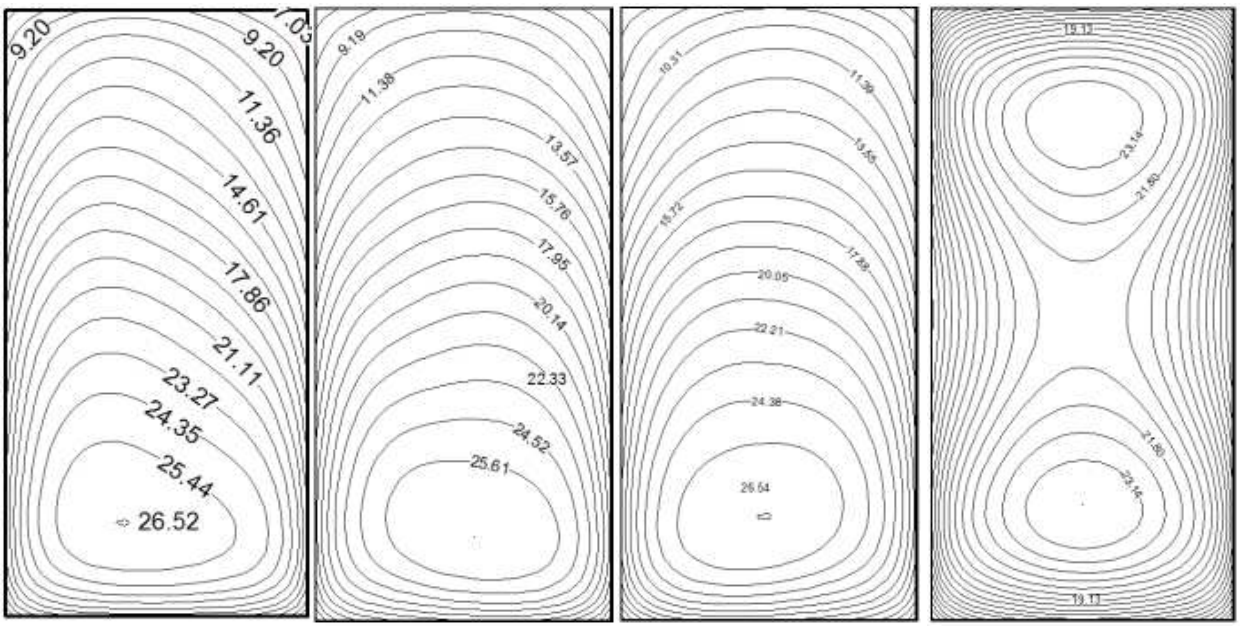

(a) (b) (c) (d)

Fig. 14. *Radiative fluxes distribution on the hot wall for γ=0° and rc= 10 and γ=0° (a), 30° (b), 60°(c) and 90°(d).*

5. Conclusion

The present numerical results are carried for $Ra=10^5$, Pr=0.71 and the optical with τ is equal to 1, Φt=0.1 and albedo equal to 1. Many conclusions are finding: in absence of radiation and by the increasing of the inclination angle of the cavity, we find that the formation of multi-roll cells is favorites.

The radiation promotes the formation of three vortex when

γ=30 ° and rather tends to make the flow mono-cellular when γ = 60 °. For γ=90°, the flow is with two contra-rotative cells for low values of rc and it is with height roll-cells when rc tends to infinite.

In absence of radiative transfer (rc=0), and by increasing the inclination angle, the isothermal surfaces are distorted and a 3D aspect appears in the core of the cavity. By the introduction of radiative fluxes, one notes the 3D distribution of the temperature for low rc number. However for higher value of rc, the temperature field becomes independent of the flow and pure radiative transfer takes place. It should be noted that the inclination of the cavity has no effect on the temperature distribution when the conductive radiative parameter goes to infinity. By increasing the inclination angle of the cavity, it is remarkable that the maximum values of the conductive heat transfer decrease and those of the radiative heat transfer increases.

Nomenclature

A – Dimension amplitude of the sinusoidal excitation
F – Aspect ratio
$\vec{g}$ – acceleration of gravity
H– height of the cavity
i– refractive index
I – dimensionless radiant intensity, $\left(=I'/(i^2\sigma(T_c')^4/\pi)\right)$
I^0– dimensionless black body intensity $\left(=I^{0\,\prime}/(i^2\sigma(T_c')^4/\pi)\right)$
L – total number of discrete solid angles
n– unit vector normal to the control volume surface
P– pressure
Pr– Prandtl number $(=\nu/\alpha)$
q_c– dimensionless local conductive heat flux on isothermal walls
q_r– dimensionless local radiative heat flux on isothermal walls
Ra– Rayleigh number
Rc– radiation conduction parameter $(=i?W.T_c^3\,\dot{\sigma}\;\lambda$
S– distance in the direction Ω of the intensity
t– dimensionless time
T– dimensionless temperature
Tc– colde temperature
Th– hot temperature
$\vec{V}$ – velocity vector
W– cavity width

Greek symbols

α– thermal diffusivity
β– extinction coefficient
β_t– coefficient of thermal expansion
ΔA– area of a control volume face
ΔV– control volume
$\Delta\Omega^l$– control solid angle
ε– emissivity
γ – inclinaition angle
ϕ_t– temperature ratio
κ – absorption coefficient
$\vec{\psi}$ – dimensionless vector potential
ϑ– kinematic viscosity
σ– Stefan–Boltzmann constant
τ– optical width
$\vec{\omega}$ – dimensionless vorticity vector
ω_0– scattering albedo
$\vec{\Omega}$ – unit vector in the direction of the intensity

Subscript

x, y, z – Cartesian co-ordinates

Superscript

'– real variables

References

[1] A. Yucel, S. Acharya and M. L. Williams: Natural convection and radiation in a square enclosure, Num. Heat Transfer 15, 261-277 (1989)

[2] Borjini M. N, Mbow C. , Daguenet M., Etude numérique du couplage rayonnement-convection naturelle en régime permanent dans des secteurs et des espaces annulaires l'aide de la méthode des volumes finis. Int. J. Therm. Sci. 38, 410-423, (1999).

[3] Borjini M. N, Ben Aissia H., Halouani K., Zeghmati B. Effect of radiative heat transfer on the three-dimensional Boyancy flow in cubic enclosure heated from the side. International Journal of Heat and Fluid Flow 29 107–118, (2008).

[4] C. Balaji, S.P. Venkateshan, Interaction of surface radiation with free convection in a square cavity, Int. J. Heat Fluid Flow 14 (3) 260–267, (1993).

[5] Chang L. C., K. T. Yang and J. R. Lloyd: Radiation natural convection interaction in two-dimensional complex enclosures, ASME J. of Heat Transfer 105, 89-95, (1983)

[6] Colomer, G., Costa, M., Cònsul, R. and Oliva A.: Three-dimensional numerical simulation of convection and radiation in a differentially heated cavity using the discrete ordinates method. Int. J. Heat Mass Transfer. 47, pp. 257-269, (2004).

[7] Desreyaud G. and G. Lauriat: Natural convection of a radiating fluid in a vertical layer, ASME J. Of Heat Transfer 107, 71--712, (1985)

[8] Henderson D., Junaidi. H., Muneer T., Grassie T., Currie J.: Experimental and CFD investigation of an ICSSWH at various inclinations. Renewable and Sustainable Energy Reviews 11, 1087–1116, (2007).

[9] Larson D.W., Viskanta R., Transient combined laminar free convection and radiation in a rectangular enclosure, J. Fluid Mech. 78 (1976) 65–85.

[10] Lioua Kolsi, Awatef Abidi, Chemseddine Maatki, Mohamed Naceur Borjini, and Habib Ben Aissia; Combined Radiation-Natural Convetion in Three-Dimensional. thermal science, Vol. 15, Suppl. 2, pp. S327-S339 (2011)

[11] Ozoe, H., Sayama, H., Churchill, S.W.: Natural convection in an inclined square channel. Int. J. Heat Mass Transfer 17 (3), 401–406, (1974).

[12] Ozoe, H., Yamamoto, K., Churchill, S.W.: Three-dimensional numerical analysis of natural convection in an inched channel with a square cross section. AICHE J. 25 (4), 709–716, (1979).

[13] Velusamy K., T. Sundararajan, K.N. Seetharamu, Interaction effects between surface radiation and turbulent natural convection in square and rectangular enclosures, J. Heat Transfer 123, 1062–1070, (2001).

[14] Wang, Q.W., Wang, G., Zeng, M., Ozoe, H.: Uni-directional heat flux through the horizontal fluid layer with sinusoidal wall temperature at the top or bottom boundaries. Int. J. Heat Mass Transfer 51 (7–8), 1675–1682, (2008).

[15] Webb B. W. and R. Viskanta: Radiation-induced buoyancy-driven flow in rectangular enclosures: experiment and analysis, ASME J. Heat Transfer 109, 427433, (1987).

[16] Yang K. T.: Numerical modelling of natural convection radiation interactions in enclosures, Int. Heat Transfer, (1986).